

Compact Waveguide-Coupled Hybrid Plasmonic Nanotaper for Optical Trapping of Nanoparticles

Yi-Chang Lin¹ and Po-Tsung Lee¹

¹ Department of Photonics, National Chiao Tung University
Room 401 CPT Building, 1001 Ta-Hsueh Road, Hsinchu 300, Taiwan
Phone: +886-988-363795 E-mail: kiraskywing@gmail.com

Abstract

We propose a waveguide-coupled hybrid plasmonic nanotaper for application of nanoparticle trapping. The features in ultra-small device footprint and ultra-low threshold power for stable nanoparticle trapping are benefit from the finely designed plasmonic mode.

1. Introduction

Recent years, sub-micron-sized particles can be precisely manipulated with low power consumption by the near-field optical tweezers [1]. It opens opportunities for particle manipulation in lab-on-a-chip system. In waveguide-coupled configuration, specific tweezer can be efficiently excited and conduct precise nanoparticle trapping [2]. If the tweezer is designed as a plasmonic structure, ultra-small device footprint and ultra-low power consumption can be achieved [3]. A potential design composed of a hybrid plasmonic nanotaper mounted on a silicon waveguide has been studied, but not been applied for optical trapping [4]. Thus, we propose a refined design and thoroughly investigated the factors which influence the trapping force. In addition, the size of the trapped particle can be selected by tuning the waveguide input power.

2. Structure Design, Operating Mechanism and Device Characteristics

The proposed design is shown in Fig. 1. To minimize the photo-damage to bioparticle, the operating wavelength is designed at 1064 nm [1]. The operating mechanism is by the following steps: 1. input the fundamental TM-like (z-polarized) silicon nitride (Si_3N_4) waveguide mode, 2. energy transfers from waveguide to nanotaper via mode beating of two excited hybrid modes, 3. highly concentrated light field at the front tip of the nanotaper via plasmonic nanofocusing [4], 4. the enhanced field intensity induces strong optical force to trap nanoparticle, as shown in Fig. 1.

We employ the 3D finite element method (Comsol Multiphysics) to explore the optical properties. The refractive indices of glass substrate, SiO_2 , Si_3N_4 , water and polystyrene sphere (PS) are 1.45, 1.45, 2, 1.33 and 1.59. The dielectric constant of the gold is fitted using Lorentz-Drude model. We fix $T_{\text{WG}} = 250$ nm, $W_{\text{WG}} = 600$ nm, $W_{\text{Au}} = 400$ nm, tip radius = 20 nm and 1 W waveguide input power in all following discussion. First, we study the relationship between L and trapping force F_z on a 100 nm in diameter PS. The nanotaper is with $t_{\text{Au}} = 20$ nm, $t_{\text{SiO}_2} = 30$ nm and the PS is at fixed position (0, 0, 65 nm). Force can be obtained by

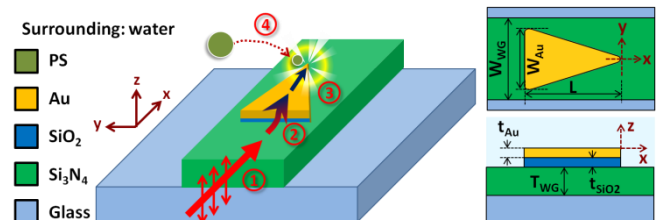


Fig. 1 Schematic illustration of the waveguide-coupled hybrid plasmonic nanotaper and its operating mechanism.

integrating a Maxwell stress tensor on the external surface of the particle [5]. The results are shown in Fig. 2(a). The short periodic variation of F_z is caused by weak Fabry-Pérot resonance, and the long one is due to mode beating (brown dash in Fig. 2(a)). A decay as L increasing is caused by the increased propagation loss. We also confirmed the operating mechanism of the optimal nanotaper with $L = 625$ nm from the electric field intensity distribution, as shown in Fig. 2(b).

Next, we set different combinations of t_{Au} and t_{SiO_2} to search the maximum $|F_z|$, as shown in Fig. 3(a). The corresponding L is also shown in Fig. 3(b). The optimal design is $t_{\text{Au}} = 20$ nm, $t_{\text{SiO}_2} = 30$ nm and $L = 625$ nm with a maximum $|F_z| = 612.7$ pN/W. To analyze the results, we examine the factors influencing $|F_z|$: transferred power to nanotaper P_T , fraction of the plasmonic mode in water f , effective mode volume in water V'_{eff} , and power enhancement G . The P_T can be calculated as $1 - \text{outflow power}$. The outflow power contains transmission, reflection and radiation loss, as shown in Fig. 4(a). When $t_{\text{Au}} = 10$ nm, the nanotaper is with small radiation, small reflection, but very large transmission. The result can be explained as a short interaction length between the waveguide mode and the nanotaper. As t_{Au} increases, the nanotaper is with decreased transmission but with increased reflection and radiation loss. The reason is that the effective index of one hybrid mode drops below the index of substrate. It not only induces larger mode mismatch

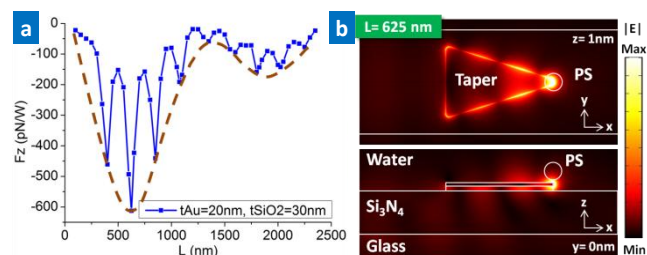


Fig. 2 (a) Optical force F_z acting on a 100 nm PS under L variation. (b) Electric field intensity distribution when $L = 625$ nm.

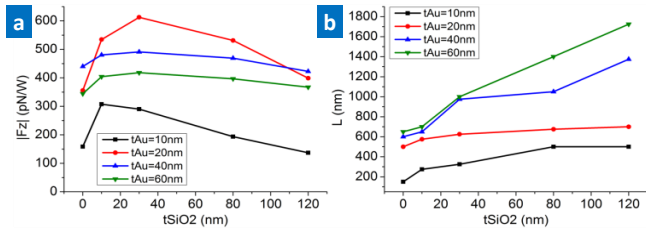


Fig. 3 (a) The optimal $|F_z|$ variation under different combinations of t_{Au} and t_{SiO_2} . (b) The corresponding optimal L .

but also mode leakage. For f , it only increases nearly proportional to t_{SiO_2} from 30% to 70%. As a larger f is, the more interaction between the PS and the mode field is. For V'_{eff} , we simply integrate the volume in water because the PS can only interact with the field in water (Fig. 4(b)). A small V'_{eff} may induce a larger gradient in light intensity, resulting in larger trapping force [1]. As t_{Au} increases, the plasmonic mode is less confined, which results in larger V'_{eff} . Furthermore, the V'_{eff} usually increases with t_{SiO_2} because L increases with t_{SiO_2} . A local minimum V'_{eff} around $t_{SiO_2} = 10$ -30 nm is due to the high confinement of hybrid mode [6]. For the G of a Fabry-Pérot cavity, it can be obtained by

$$G = 1 + \alpha^2 + \alpha^4 + \dots = \frac{1}{1 - \alpha^2}, \alpha = \exp(-2 \int k'(W, t_{Au}, t_{SiO_2}) \cdot dL) \quad (1)$$

where α is the propagation loss of the plasmonic mode on the nanotaper. k' is the imaginary part of propagation constant of the mode, which is a function of taper width W , t_{Au} and t_{SiO_2} . After one round trip, the power would become α^2 . As shown in Fig. 4(c), G is increased with t_{Au} due to a smaller k' , and usually decreases with t_{SiO_2} because L increases with t_{SiO_2} that results in larger propagation loss. A local maximum G around $t_{SiO_2} = 10$ -30 nm is caused by the small k' of hybrid mode [6]. To combine all the factors above, we introduce a force factor F defined as $P_T \times f \times G / V'_{eff}$, as shown in Fig. 4(d). The trend of F similar to Fig. 3(a) proves that the $|F_z|$ is indeed influenced by these factors. However, the estimation of α is not very accurate, causing some mismatch between Fig. 4(d) and Fig. 3(a).

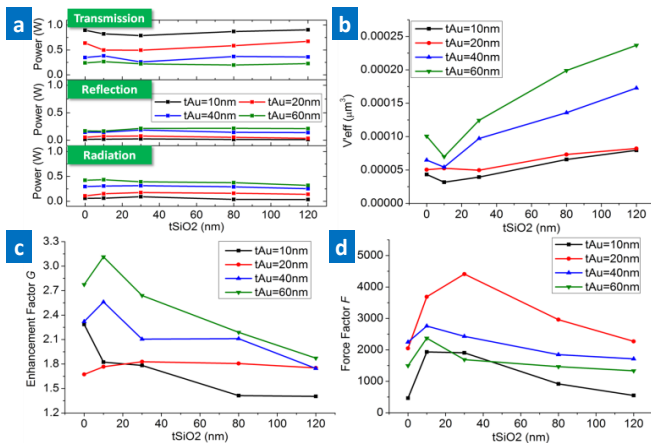


Fig. 4 The analysis of the nanotaper: (a) transmission, reflection, and radiation power, (b) V'_{eff} , (c) G factor, and (d) F factor.

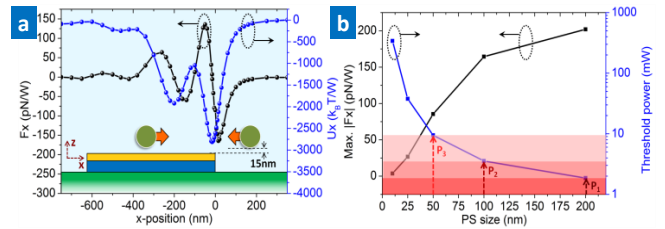


Fig. 5 (a) Trapping force F_x and potential U_x on a 100 nm PS as a function of x position at $z = 65$ nm. (b) The maximum $|F_x|$ and threshold power of different PS sizes from 10 nm to 200 nm.

3. Force Analysis and Trapping Particle of Specific Size

Assuming that a 100 nm PS is trapped at the top surface of the optimal nanotaper with a 15 nm separation ($z = 65$ nm), we map the horizontal force F_x along x -direction. Then, the potential U_x experienced by the PS can be calculated by integrating F_x along the path, as shown in Fig. 5(a). There is always a force pulling the PS towards two stable positions at $x = -15$ nm with $U_x = -2813$ $k_B T/W$ and $x = -200$ nm with $U_x = -1922$ $k_B T/W$. A widely used criterion for stable trapping is $10k_B T$ for suppressing Brownian motion [7]. Thus, an ultra-low threshold power of 3.6 mW is sufficient for stable trapping of a 100 nm PS. We also calculate the maximum $|F_x|$ and the threshold power for different PS sizes from 10 nm to 200 nm, as shown in Fig. 5(b). Because the $|F_x|$ decreases rapidly as the PS size decreases, a larger threshold power for trapping tiny PS is needed. Thus, the size of the trapped particle can be selected by tuning input power.

4. Conclusions

In summary, we proposed a waveguide-coupled hybrid plasmonic nanotaper operating at wavelength of 1064 nm with less photo-damage to bioparticle. All factors that influence the trapping force strength provided by the nanotaper have been thoroughly investigated, and can be combined into a force factor F . An optimal nanotaper is with $t_{Au} = 20$ nm, $t_{SiO_2} = 30$ nm and $L = 625$ nm. The device is more compact compared to a pure dielectric one [2]. We showed that stable trapping a 100 nm PS can be achieved with threshold power of merely 3.6 mW. Furthermore, the size of trapped particle can be selected by tuning input power. We believe that this design can improve the development of nano-bio-target manipulation in lab-on-a-chip system.

Acknowledgement

This work is supported by Taiwan's Ministry of Science and Technology (MOST) under contract number MOST-103-2221-E-009-096-MY3.

References

- [1] D. Erickson, *Lab Chip* **11** (2011) 995.
- [2] P. Kang *et al.*, *Sci. Rep.* **5** (2015) 12087.
- [3] M. L. Juan *et al.*, *Nat. Photonics* **5** (2011) 349.
- [4] Y. Luo *et al.*, *Nano Lett.* **15** (2015) 849.
- [5] A. H. J. Yang and D. Erickson, *Nanotechnology* **19** (2008) 045704.
- [6] D. Dai and S. He, *Opt. Express* **17** (2009) 16646.
- [7] A. Ashkin *et al.*, *Opt. Lett.* **11** (1986) 288.